Original Article

Journal of Green Development Management Studies

2025, Volume 4, Special Issue, Pages 111-126

https://doi.org/10.22077/jgdms.2025.8670.1239

Evaluating the Role of Urban Green Spaces in Reducing Vulnerability and Enhancing Climate Resilience in Zahedan

Fatemeh Yadegari Far[1], Seyed Hossein Mirmousavi[2*], Mohammadreza Poudineh[3]

1. PhD Candidate in Climatology, Department of Geography, University of Zanjan, Zanjan, Iran
2. Associate Professor of Climatology, Department of Geography, University of Zanjan, Zanjan, Iran
3. Associate Professor of Climatology, Department of Geography, University of Sistan and Baluchestan, Zahedan, Iran

*Corresponding author, Email: hossein.mirmousavi@znu.ac.ir

Keywords:
Remote Sensing, Resilience, Zahedan, Vulnerability, Green Spaces.

Abstract

In the face of escalating climate change and its cascading impacts, urban resilience has become a fundamental approach to achieving sustainable city management. Zahedan, situated in an arid to semi-arid region, experiences severe climatic stressors including rising land surface temperatures, declining soil moisture, intensifying droughts, and increasing occurrences of dust storms. This study investigates the role of urban green spaces in reducing climate vulnerability and enhancing resilience, focusing on two neighborhoods with contrasting environmental conditions: Daneshgah (University) and Shirabad. Utilizing Landsat satellite imagery, spatiotemporal changes in vegetation cover (NDVI) and land surface temperature (LST) were analyzed for the period 1980–2023. Climatic parameters—air temperature, precipitation, humidity, and wind speed—were examined through time-series analysis and validated using the Mann–Kendall trend test. Furthermore, the TOPSIS multi-criteria decision-making model was applied to evaluate and rank neighborhood vulnerability and resilience levels. The results reveal a marked decline in vegetation cover accompanied by a significant rise in land surface temperature over the past four decades. Drought indices suggest that decreasing precipitation and humidity levels are primary drivers of these patterns. The Daneshgah neighborhood, characterized by greater vegetation density, exhibits higher climate resilience compared to Shirabad. Vegetation in Daneshgah enhances urban resilience by absorbing carbon dioxide, releasing oxygen, reducing ambient temperature, and improving soil water retention, thereby mitigating air pollution and urban heat island effects. Conversely, Shirabad's compact built environment, inadequate infrastructure, and limited green space intensify its climate vulnerability. The findings underscore the critical role of effective green space management—particularly through the cultivation of drought-tolerant species, adoption of smart irrigation technologies, and establishment of urban green belts—in strengthening Zahedan's urban climate resilience.

Received:
31/Dec/2024

Revised:
28/Feb/2025

Accepted:
27/May/2025

How to cite this article:

Yadegari Far, F., Mirmousavi, S.H. & Poudineh, M.R. (2025) Evaluating the Role of Urban Green Spaces in Reducing Vulnerability and Enhancing Climate Resilience in Zahedan. *Green Development Management Studies*, **4(Special Issue), 111-126. https://doi.org/10.22077/jgdms.2025.8670.1239**

Introduction

Green spaces are among the most vital components of urban environments, playing a critical role in enhancing resilience against natural hazards particularly drought and climate change. This function is realized through mechanisms such as moderating air temperatures, improving air quality, controlling urban flooding, preserving biodiversity, and promoting the mental well-being of city residents (Hesari, 2023, p. 68). In arid and semi-arid regions such as Zahedan, green spaces can help mitigate the effects of drought by reducing evaporation and increasing soil permeability, thereby facilitating better water resource management. Furthermore, urban vegetation contributes to dust control by stabilizing soil and decreasing wind velocity (Eskandari Sani et al., 2023, p. 89). Due to its specific geographical location, Iran is highly exposed to numerous natural hazards. Out of the 40 globally recognized natural hazards, 31 occur within the country (Nowruzi, 2019, p. 74). The average annual precipitation in Iran is approximately 250 mm roughly one-third of the global average. In recent decades, the country has experienced some of its most prolonged and severe droughts. Simultaneously, water consumption in Iran has consistently exceeded the initial water stress threshold (Afrakhteh & Hajipour, 2024, p. 46). Under such circumstances, effective drought management in arid and semi-arid areas like Iran becomes critically important. Traditional crisis management approaches mainly reactive, focused on emergency response and post-disaster government aid have proven insufficient in reducing long-term vulnerability and have instead increased the dependency of local communities (Malekan et al., 2020, p. 728). In contrast, the urban resilience approach, which emphasizes enhancing the capacity of communities to cope with disasters, has emerged as a more effective framework for addressing climate-related crises (Milleti, 1999, p. 172). In this context, the present study examines the role of green spaces in reducing climate vulnerability and enhancing resilience in two neighborhoods of Zahedan: Daneshgah (University) and Shirabad. The primary aim is to analyze the impact of vegetation cover on climate moderation, the mitigation of drought and urban heat effects, and overall improvement in environmental quality.

Theoretical Framework

Urban resilience refers to the capacity of a community to absorb, adapt to, and recover from natural hazards and climate-related disruptions (Adger et al., 2005, p. 1036). Initially rooted in the field of disaster risk management, this concept has since evolved into a cornerstone of sustainable urban planning (Parry et al., 2009, p. 76). Climate resilience specifically encompasses a set of preventive and adaptive strategies aimed at reducing vulnerability and enhancing the ability of cities to cope with climate change. Among the various tools for fostering climate resilience, urban green spaces are considered one of the most effective. Vegetation plays a critical role in moderating the urban climate by lowering ambient temperatures, improving air quality, increasing soil water retention, reducing evaporation, and capturing atmospheric carbon dioxide (Nowak & Crane, 2000, p. 718). These ecological services contribute to mitigating the adverse effects of climate change and improving overall urban environmental quality (Alberti, 2005, p. 198). Climate resilience indices serve as essential tools for assessing the vulnerability of different regions. These indices integrate environmental, social, and economic factors to evaluate a region’s capacity to withstand and adapt to climatic stresses (Sullivan & Meigh, 2005, p. 70). Within this context, sustainable green space management including the selection of drought-resistant plant species, the development of green belts, and the implementation of smart irrigation systems is widely recognized as a key strategy in enhancing urban resilience.

Urban resilience to climate change has emerged as a key concept in sustainable development and has been widely examined in numerous studies. Early research in this field primarily focused on disaster management and reducing the damage caused by natural hazards. For instance, Mileti (1999, p. 203) emphasized the need to replace traditional, reactive crisis responses with resilience-based strategies. He argued that establishing robust infrastructure including the development of green spaces can serve as a critical tool in addressing climate-related risks.

Sullivan and Meigh (2005, p. 75), in their analysis of climate vulnerability indices, highlighted the significance of environmental, social, and economic factors in shaping community resilience to climate change. Their findings suggest that green spaces play a crucial role in reducing vulnerability by increasing relative humidity, improving air quality, and moderating ambient temperatures. In line with this, Alberti (2005, p. 192) explored the relationship between urban spatial patterns and ecosystem performance, demonstrating that the distribution of green spaces significantly reduces urban heat intensity while enhancing urban ecological structure.The environmental and social health benefits of green infrastructure have also attracted research attention. Landry and Chakraborty (2009, p. 2668) found that the expansion of green spaces in urban areas not only enhances climate resilience but also fosters social cohesion and reduces inequality, thereby improving overall quality of life. Similar conclusions were drawn by Nowak and Crane (2002, p. 718), who underlined the importance of vegetation in mitigating air pollution and enhancing ecological quality.

In recent years, attention has increasingly turned toward the multifaceted role of urban green infrastructure in sustainable climate adaptation. McPherson et al. (2018, p. 592) investigated the role of biodiversity in enhancing resilience within urban systems. Their study concluded that multifunctional green spaces featuring a mix of drought-tolerant species and shade trees can significantly alleviate heat stress. Farini et al. (2020, p. 19) also emphasized the importance of sustainable green space management in reducing climate change impacts. Their findings indicate that urban vegetation plays a pivotal role in lowering ambient temperatures, capturing airborne pollutants, managing stormwater runoff, and decreasing noise pollution, thereby strengthening urban resilience. Smart planning and sustainable maintenance of green spaces through biodiversity preservation and species selection adapted to climate stress can improve urban living standards while mitigating global warming. These insights are echoed in a study by Gherri (2023, p. 11), which showed that urban vegetation significantly contributes to mitigating heat in densely populated areas. By providing shade and improving air circulation, green spaces reduce ambient temperatures and increase thermal comfort. The study also noted that interactions between vegetation and urban morphology can produce varying effects on surface temperature reduction. Continuing this line of inquiry, Zhang et al. (2025, p. 22) demonstrated that urban vegetation plays a key role in reducing fire risk under changing climate conditions. Through physical barriers and reduced flammability, plants limit fire spread and enhance urban resilience. The study also emphasized that plant diversity and sustainable green space management can substantially reduce the intensity of urban wildfires.

In the Iranian context, several studies have explored the role of green spaces in climate resilience. Nowruzi (2019, p. 85), in a study on rural settlement resilience, noted relatively strong performance in social and physical dimensions, but highlighted severe vulnerability in economic and managerial aspects. His findings stressed that expanding green infrastructure in rural areas can enhance livelihood resilience. Yadegari Far et al. (2023, p. 345) investigated Zahedan's vulnerability to water crises and drought, concluding that declining water resources and increasing dust storms have adversely affected the region's social and economic well-being. Their study underlined the potential of urban green spaces especially in water-scarce regions like Zahedan to alleviate the harmful effects of climate change. Similarly, Malekan et al. (2020, p. 716) criticized traditional crisis response policies in Iran, arguing they are ineffective for long-term vulnerability reduction. They advocated for resilience-based strategies, emphasizing the role of drought-tolerant species, green belts, and expanded green spaces around cities as effective climate adaptation tools. In a remote sensing-based study, Golestani et al. (2022, p. 341) analyzed the relationship between vegetation cover and land surface temperature in Isfahan. Their findings confirmed that areas with greater green space experience lower surface temperatures and reduced urban heat island effects. Overall, both international and domestic studies consistently support the conclusion that sustainable development and management of green spaces can significantly enhance climate resilience. The present research uses satellite imagery, climate data analysis, and the TOPSIS modeling approach to examine the impact of green spaces on climate resilience in two Zahedan neighborhoods: Daneshgah and Shirabad. It aims to provide scientifically grounded strategies to improve green space policy and management in this region.

Given the environmental significance of Daneshgah and Shirabad, it is essential to assess the impact of drought and dust storms on their climate resilience. Drought, as one of the most severe climate hazards, contributes to water scarcity, soil erosion, and vegetation degradation, thereby increasing dust storm activity. This phenomenon rooted in unsustainable development and poor environmental management has far-reaching effects on local ecosystems, air quality, and public health. Dust storms exacerbate particulate pollution, disrupt ecological systems, and pose a major threat to urban infrastructure, economic productivity, and environmental sustainability. If such conditions persist, they could accelerate desertification, reduce ecological carrying capacity, and intensify regional environmental risks. This study examines drought and dust storm effects from both climatological and natural hazard perspectives, assessing the resilience of the target area in the face of these growing challenges.

Materials and Methods

This study employs both quantitative and qualitative data. Initially, a comprehensive literature review was conducted using academic sources, including books, peer-reviewed articles, theses, and official reports, to gather background information relevant to the research topic. Existing theories and conceptual frameworks related to urban resilience were examined to establish a theoretical foundation.To address the research questions and fulfill the study's objectives, a structured questionnaire was developed based on the expected dimensions of climate resilience. This questionnaire was distributed across the study area and completed by a range of participants, including local experts, university professors, technical specialists, and residents of Zahedan. The collected responses were then analyzed to extract insights into perceived vulnerabilities and adaptation capacities.Following this, key indicators and criteria influencing the assessment of neighborhood-level resilience to climate change in Zahedan were identified. These indicators served as the basis for evaluating how different urban areas respond to environmental stressors and the role of green spaces in enhancing or limiting their resilience.

Study Area

Zahedan, the capital of Sistan and Baluchestan Province, is located in southeastern Iran at approximately 29°28' N latitude and 60°53' E longitude. The city spans an area of roughly 41,400 square kilometers and is characterized by a hot and arid climate. It receives one of the lowest annual precipitation rates in the country, with an average of less than 100 millimeters. In addition to experiencing extreme drought and chronic water scarcity, Zahedan is exposed to frequent dust storms, sandstorms, and rising land surface temperatures due to its geographical position. These environmental stressors have a direct impact on both the quality of life and ecological sustainability of the region (Poudineh et al., 2020, p. 135). Urban green space coverage in Zahedan is significantly below both national and international standards. The current per capita green space is approximately 4 square meters per person, whereas the national average in Iran ranges between 8 to 12 square meters, and global standards suggest a minimum of 20 to 25 square meters per person (Manouchehri et al., 2011, p. 27). The city's vegetation primarily consists of drought-resistant tree species such as Prosopis (Kahoor), Tamarix (Gaz), Eucalyptus, Conocarpus, and various types of palms. These species are mainly distributed across limited urban areas, including parks, street edges, and educational institutions. However, the spatial distribution of green spaces is highly uneven, and many zones particularly informal or marginalized neighborhoods such as Shirabad lack adequate green coverage. Figure 1 illustrates the geographical location of the studied neighborhoods and highlights the spatial distribution of vegetation cover in Zahedan using green overlays.

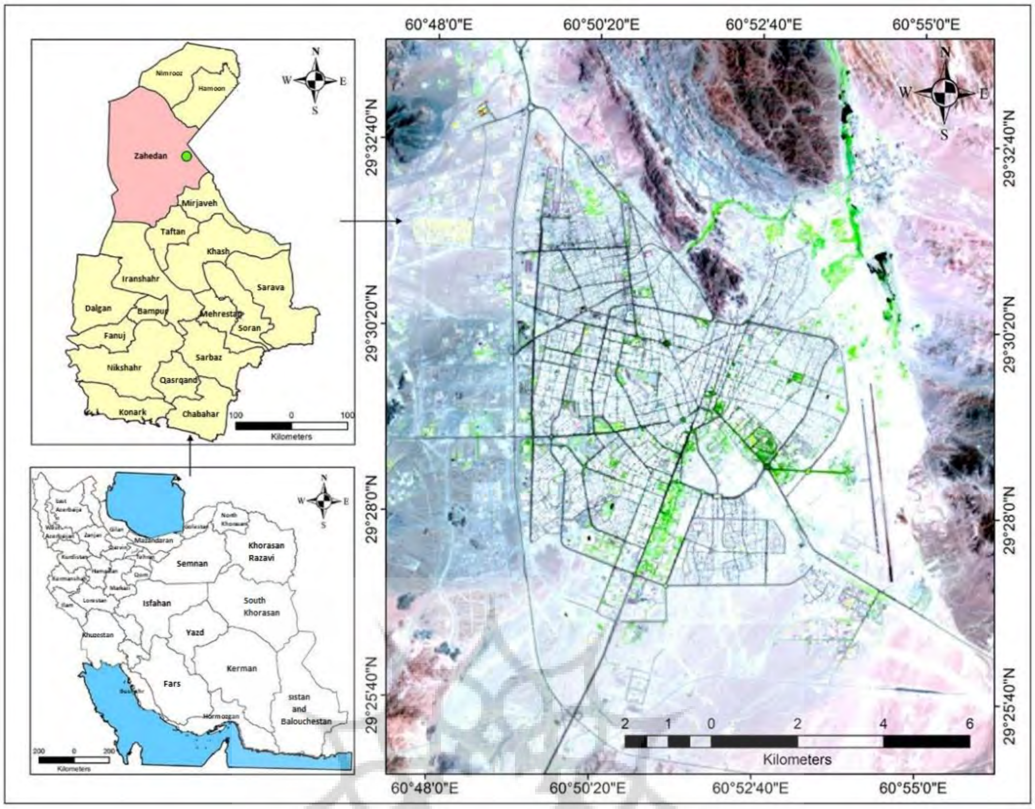

Figure 1. Geographic location of the selected neighborhoods within the city of Zahedan.

Research Findings

In this study, meteorological data from the Zahedan synoptic weather station including humidity, wind speed and direction, dust concentration, precipitation, and temperature were used to assess climate change trends. The data were collected based on monthly observations from synoptic records over a 42-year period (1981 to 2022). To analyze trends in key meteorological parameters such as precipitation, temperature, and other climatic variables, time series analysis and the non-parametric Mann-Kendall trend test were employed. Data processing and statistical analyses were conducted using SPSS software to ensure accuracy and consistency in the interpretation of climatic trends.

Trend Analysis Using the Mann-Kendall Test

The Mann-Kendall test is a non-parametric rank-based method suitable for detecting both linear and non-linear trends in time series data (Makkari & Abbasnia, 2020, p. 35). It is particularly useful for identifying monotonic trends either increasing or decreasing without the assumption of normal data distribution. The method begins by computing the difference between all data pairs within the time series. Then, using a sign function (*sgn*), the test statistic is calculated based on the following formula (Equation 1), as proposed by Helsel and Hirsch (2002, p. 217):

$$S = \sum_{k=1}^{n-1} \sum_{j=k+1}^{n} sgn(x_j - x_k) \quad (1)$$

In Equation 1, n represents the total number of observations in the time series; *xj* denotes the *j*-th data point, and *xk* denotes the k-th data point in the same series.

The sign function (*sgn*) is a simple yet essential mathematical tool used to determine the direction or trend between two values. It compares two observations and indicates whether the second value has increased, decreased, or remained unchanged relative to the first. The output of this function is either +1, 0, or −1, corresponding to an increase, no change, or a decrease, respectively. The sign function is defined as follows:

$$Sgn(x) = \begin{cases} +1 & if \quad (x_j - x_k) > 0 \\ 0 & if \quad (x_j - x_k) = 0 \\ -1 & if \quad (x_j - x_k < 0 \end{cases} \tag{2}$$

The Non-Parametric Sen's Slope Estimator

The Sen's Slope Estimator is a non-parametric method used to estimate the linear trend in a time series. Originally introduced by Theil in 1950 and later developed by Sen in 1968, this method, like the Mann-Kendall test, is based on the analysis of pairwise differences between data points in a time series. It is particularly appropriate when the underlying trend is assumed to be linear over time (Gadgisu Toso et al., 2023, p. 5). This method estimates the median of all possible slopes between data point pairs and provides a robust, distribution-free measure of trend magnitude. It is applicable when the function f*(t)*, representing the trend over time, is linear. As shown in Equation 3, the model is defined as follows:

$$f(t) = Qt + B \tag{3}$$

In Equation 3, Q represents the slope of the trend line, while B is the intercept constant.

To compute the trend slope Q, the slope between all possible pairs of observed data points is calculated using the following formula, presented as Equation 4:

$$Q = \frac{x_j - x_k}{j - k} \tag{4}$$

In Equation 4, *j>k*. In this equation, *xj* and *xk* represent the observed data at times *j* and *k*, respectively. By applying this equation, a slope was obtained for each pair of observed data. By placing these slopes together, a time series of calculated slopes was formed. That is, if there are *n* values of *xj* in the time series, then *N=n(n−1)/2* slope estimates (*Qi)* are obtained.

In the next step, the median of the studied time series was calculated. For this, the *N* values of (*Qi*) were sorted in ascending order, and then, using one of the following equations, the median of the time series was determined. If the number of observations in the time series was odd, Equation (5) was used, and if even, Equation (6) was used (Gonzalo, 2004, p. 89).

$$Q = Q_{[(N+1)/2]} \tag{5}$$

$$Q = \frac{1}{2}\left[Q_{[N/2]} + Q_{[(N+2)/2]}\right] \tag{6}$$

The result obtained from these equations was the slope of the trend line (*Qmed*). If the slope of the trend line was positive, it indicated an increasing trend, and if negative, it indicated a decreasing trend in the data.

In this study, the next step was to test the obtained slope at a 95% confidence interval. To perform this test, the following equation was used:

$$C_a = Z_{1-a/2}\sqrt{VAR(S)} \tag{7}$$

In Equation 7, *Z* represents the standard normal distribution statistic in a two-tailed test, which for a 95% confidence level is equal to *Z=1.96*, and *VAR(S)* is the variance of the parameter *S*. To calculate the value of the parameter *S* as well as *VAR(S)*, the following steps were taken (Alijani et al., 2011, p. 26):

a) Calculating the difference between each element in the time series and all others, applying the sign function (sgn), and deriving the parameter SSS using the following formula:

$$S = \sum_{k=1}^{n-1}\sum_{j=k+1}^{n} sgn(x_j - x_k) \tag{8}$$

In the above equation, n is the number of observations in the series, and xj and xk are the j-th and k-th data points in the series, respectively.

b) Calculation of the sign function (sgn), which was computed as follows:

$$Sgn(x) = \begin{cases} +1 & if \quad (x_j - x_k) > 0 \\ 0 & if \quad (x_j - x_k) = 0 \\ -1 & if \quad (x_j - x_k < 0 \end{cases} \tag{9}$$

c) Calculation of the variance of S using one of the following equations. If the number of data points in the time series is greater than 10, Equation (3-11) was used; if fewer than 9, Equation (3-12) was applied.

$$VAR(S) = \frac{n(n-1)(2n+5) - \sum_{i=1}^{m} t(t-1)(2t+5)}{18} \tag{10}$$

$$VAR(S) = \frac{n(n-1)(2n+5)}{18} \tag{11}$$

In the above equation, n is the number of observed data points, m is the number of tied groups in which at least one repeated value occurs, and ttt represents the frequency of data with identical values.

Finally, the upper and lower confidence limits were calculated using the following formulas:

$$\begin{cases} M_1 = \frac{n' + C_a}{2} \\ M_2 = \frac{n' - C_a}{2} \end{cases} \tag{12}$$

Based on the above formula, the *M1-th* and *M(2+1)-th* slope values were extracted from among the calculated slopes. If the value zero fell within the range between these two slope values, the null hypothesis was accepted and the absence of a trend in the data series was confirmed. Otherwise, the null hypothesis was rejected, indicating the presence of a statistically significant trend at the tested confidence level.

Finally, to obtain the value of B in Equation (3-4), the differences $xi{-}Qti$ were calculated for all n observations. The median of these values was then used to estimate B (Alijani et al., 2011, p. 27).

Standardized Precipitation Index (SPI)

Drought is one of the most complex climatic phenomena, and its analysis requires consideration of multiple characteristics such as severity, intensity, and duration. In 1993, researchers at the University of Colorado introduced the Standardized Precipitation Index (SPI) as a tool for drought monitoring, which has since become a key instrument for early warning systems and the assessment of drought severity (McKee et al., 1993, p. 179). Since precipitation data typically do not follow a normal distribution, calculating this index requires fitting appropriate probability distributions to the observed data. Studies have shown that the choice of distribution varies across regions and has a direct impact on the accuracy of the index calculations (Shahabfar & Eitzinger, 2013, p. 99). By standardizing precipitation data, SPI enables the comparison of drought conditions across different locations and plays a significant role in water resource management. In this study, the following formula was used to calculate the intensity and duration of drought episodes (Guttman, 1999, p. 315):

$$spi = \frac{pi - \bar{p}}{s} \tag{13}$$

In the above equation, pi represents the precipitation during the studied period, $\bar{p}$ denotes the long-term average precipitation for that period, and S is the standard deviation of precipitation values.

The classification of drought and wetness conditions based on SPI values was introduced by McKee (Table 1). Positive SPI values indicate precipitation above the long-term mean, while negative values indicate the opposite. According to this method, a drought period is defined as any span during which the SPI remains continuously negative and falls to –1 or below. The drought is considered to end when the SPI value becomes positive again. The cumulative SPI values reflect the magnitude and severity of the drought episode.

Table 1. Classification of Drought and Wetness Severity Using the Standardized Precipitation Index (SPI)

SPI Value Range	Category
SPI ≥ +2.00	Extremely Wet
+1.50 ≤ SPI < +1.99	Severely Wet
+1.00 ≤ SPI < +1.49	Moderately Wet
−0.99 ≤ SPI ≤ +0.99	Near Normal
−1.49 ≤ SPI < −1.00	Moderately Dry
−1.99 ≤ SPI < −1.50	Severely Dry
SPI ≤ −2.00	Extremely Dry

(Source: McKee et al., 1995, p. 234)

In this study, trends in vegetation cover and land surface temperature (LST) were analyzed using a time series of Landsat satellite imagery. For this purpose, data from Landsat 4, 5, and 8 were acquired from the United States Geological Survey (USGS) and stored in a unified geospatial database. Subsequently, geometric and radiometric corrections were applied using GIS and ENVI software. The analysis focused on changes in vegetation and surface temperature over a 44-year period (1980–2023). Two indices were extracted for the Zahedan urban area: the Normalized Difference Vegetation Index (NDVI) and Land Surface Temperature (LST). Landsat images were selected at ten-year intervals, specifically from the years 1980, 1990, 2000, 2010, 2020, and 2023, chosen based on their suitable spatial resolution (see Table 2).

All images were processed in ENVI software and georeferenced to the Inverse Mercator projection system using the nearest neighbor resampling method (Hao et al., 2012, p. 391). This process enabled precise analysis of vegetation and surface temperature trends over the past four decades.

Table 2. Number of Selected Satellite Images Used in Each Month of the Study Period

Band Description	Landsat 8 OLI	Spectral Range (μm)	Spatial Resolution (m)	Landsat 5 ETM+	Landsat 4 ETM	Spectral Range (μm)	Spatial Resolution (m)	Year
Coastal aerosol	Band 1	0.43–0.45	30					
Blue	Band 2	0.45–0.51	30	0.50–0.60	30			1980
Green	Band 3	0.53–0.59	30	Band 2	Band 2	0.60–0.70	30	
Red	Band 4	0.64–0.67	30	Band 3	Band 3	0.70–0.80	30	1990
Near-Infrared (NIR)	Band 5	0.85–0.88	30	Band 4	Band 4	0.80–1.10	30	2000
SWIR 1	Band 6	1.57–1.65	30	Band 5	Band 5	1.10–1.30	30	2010
SWIR 2	Band 7	2.11–2.29	30	Band 6	—	—	30	2020
Panchromatic	Band 8	0.50–0.68	15	Band 7	—	—	30	2023
Cirrus	Band 9	1.36–1.38	30	—	—			

(https://landsat.gsfc.nasa.gov/multispectral-scanner)

Normalized Difference Vegetation Index (NDVI)

Green vegetation absorbs the highest amount of solar radiation in the visible portion of the electromagnetic spectrum, whereas it reflects more strongly in the near-infrared (NIR) range. Satellite imagery, by measuring the reflectance of red and NIR light (approximately 0.58–0.68 μm and 0.73–1.10 μm, respectively), provides valuable information on vegetation cover. This data is used to assess plant growth, estimate biomass, and evaluate vegetation health. To quantify and analyze vegetation properties, researchers use vegetation indices mathematical formulas that compare the reflectance intensity in different spectral bands, particularly red and NIR. Since vegetation strongly absorbs red light and reflects NIR, the contrast between these two bands provides critical insights into plant condition (Khosravi Yeganeh et al., 2024, p. 86).

The vegetation index plays a key role in energy exchange between the atmosphere and Earth's surface, influencing various climatic factors, including ambient temperature. Therefore, it is also a significant input in the calculation of Land Surface Temperature (LST). In this study, Band 4 (Red) and Band 5 (NIR) of the Landsat satellite were used to calculate the NDVI. The index was computed using Equation (14) as follows (Najafi et al., 2020, p. 261):

$$NDVI = (Band^5 - Band^4)(Band^5 + Band^4) \quad (14)$$

NDVI values range from –1 to +1. High reflectance in the near-infrared region of the electromagnetic spectrum indicates plant health, with high values between 0.05 and 1 (Sarani & Hashemi, 2023, p. 80). In this index, numerical values between 0.1 and 0.5 correspond to areas with sparse vegetation, 0.5 to 0.6 for areas with moderate and semi-dense vegetation, and 0.6 to 0.7 for areas with very dense and lush vegetation. Water, snow, and ice have negative NDVI values, and soils also show values less than 0.05. Clouds generally have NDVI values equal to zero (Hosseini Chamani et al., 2019, p. 245).

Vegetation Cover Map Analysis (NDVI)

In this study, vegetation cover maps derived from processed Landsat satellite imagery for the month of July from 1980 to 2023 were prepared to examine the temporal trends in vegetation across the study area (Figure 2). July was selected as it represents the hottest month of the year and is thus critical for assessing vegetation resilience. According to the correlation analyses and as clearly visible in the maps vegetation cover throughout the study period has remained sparse and scattered. Analysis of precipitation, temperature, and humidity data indicates that limited rainfall and air moisture, combined with high regional temperatures, are the main environmental constraints on vegetation density. A comparison between Shirabad neighborhood (in the north of the city) and the University neighborhood (in the south) reveals that, historically, Shirabad had denser vegetation due to its peripheral location. However, over time particularly with the expansion of the University area as the city's academic hub this trend has reversed. The decline in vegetation in Shirabad can be attributed to large-scale construction, unregulated growth of informal settlements, and destruction of natural green cover. In contrast, the increase in vegetation within the university compound is the result of urban development projects and deliberate green space expansion. These changes underscore the influence of human activities, urban development, and climatic conditions on the distribution and sustainability of vegetation in the region.

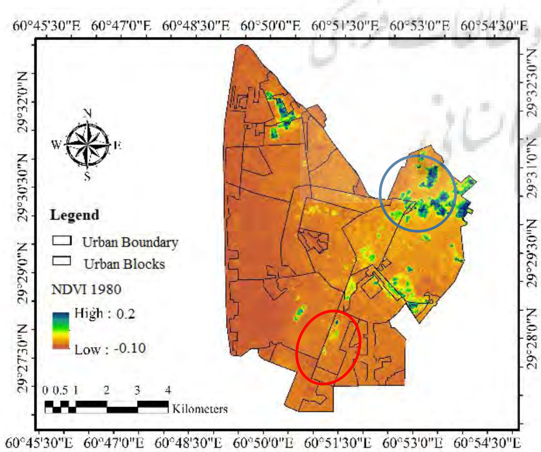

1980

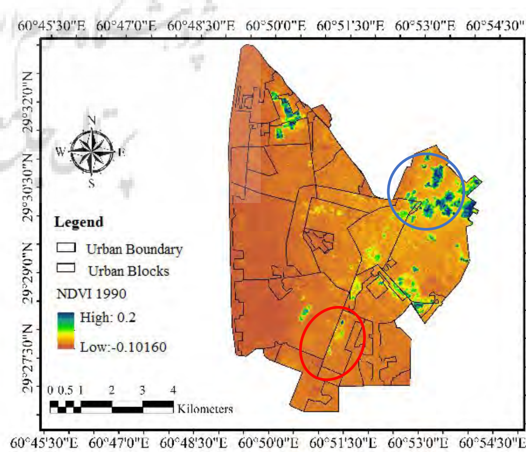

1990

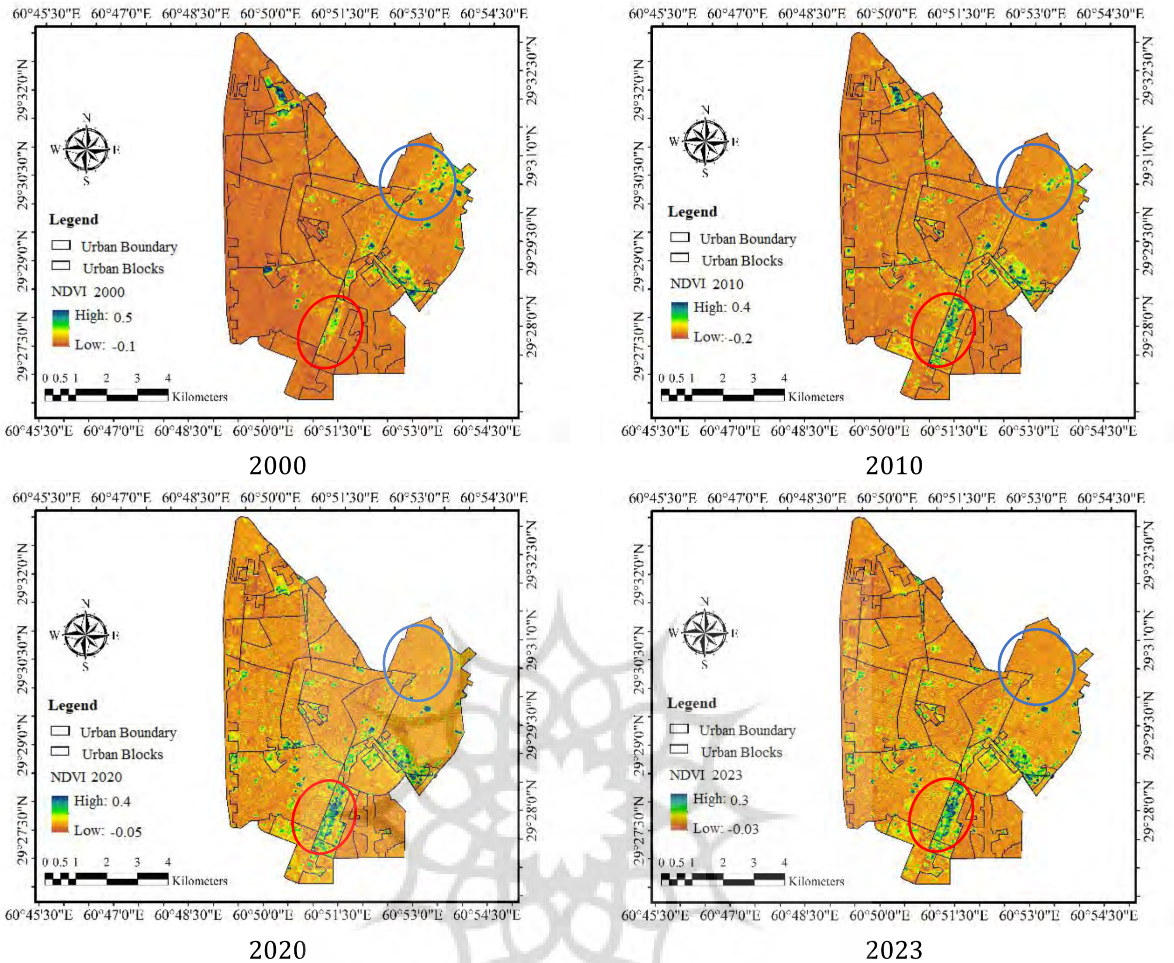

Figure 2. NDVI Vegetation Cover Maps of Zahedan for the Month of July during the 1980–2023 Period

Land Surface Temperature (LST) Map Analysis

In the present study, Landsat images for the month of July in Zahedan were obtained from the NASA archive for the years 1980 to 2023. These images were used to generate Land Surface Temperature (LST) maps for July over the specified time period (Figure 3). The spatial variability of surface temperatures across Zahedan County is clearly observable in these maps. In 2023, the maximum recorded land surface temperature reached 48.5°C, whereas in 1980, the maximum temperature was only 23.6°C. This comparison alone indicates a significant rise in temperature over the period, primarily attributed to the decline in rainfall in Zahedan during this time. Furthermore, the spatial distribution of land surface temperatures shows that Shirabad neighborhood, located in the northern elevated areas of the city, consistently exhibits lower LST values compared to the University neighborhood in the south. However, between 2010 and 2023, despite generally higher temperatures in the University area, parts of this neighborhood showed lower surface temperatures than Shirabad, due to the increase in vegetation cover around the university campus.

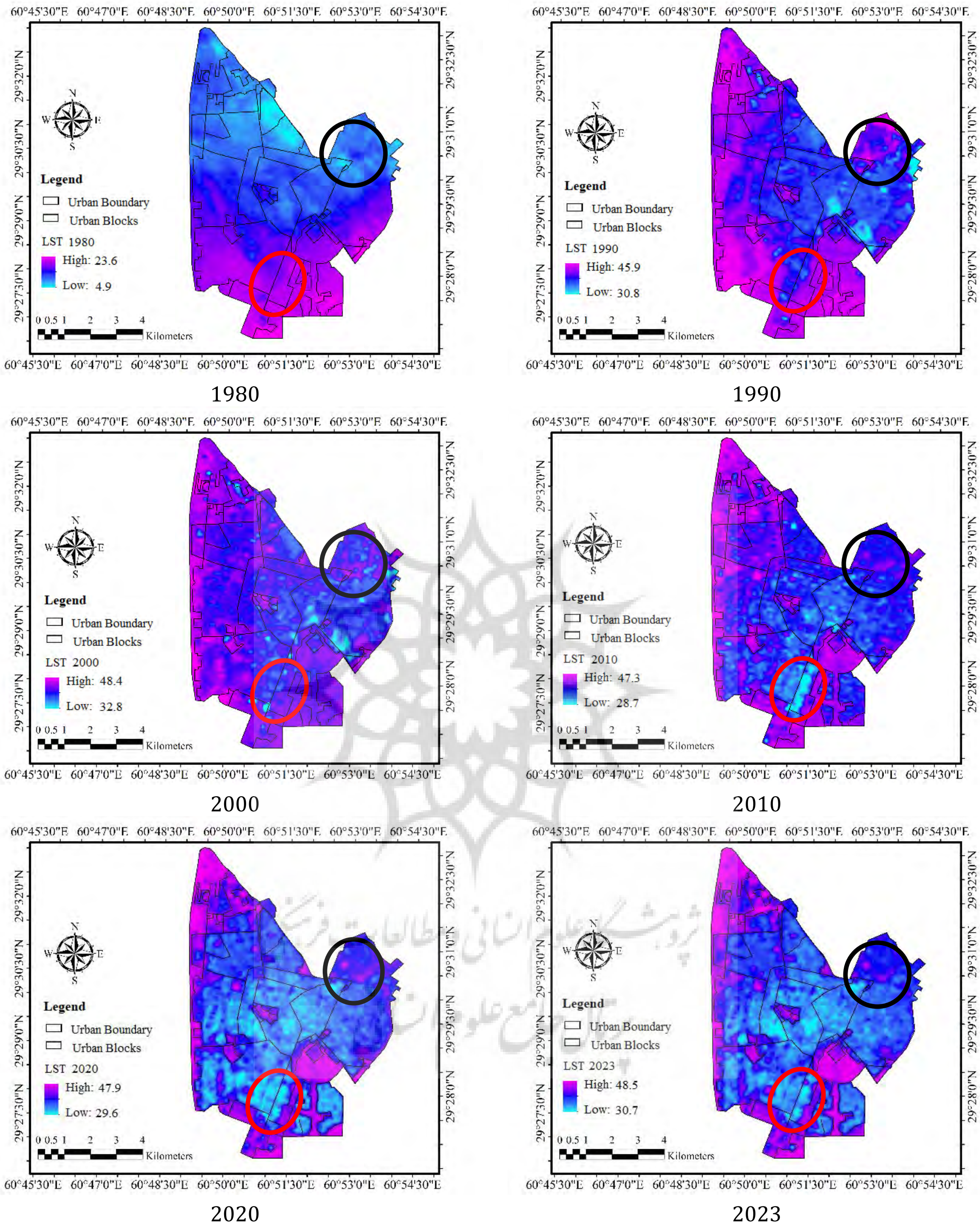

Figure 3. Land Surface Temperature (LST) Maps of Zahedan for the Month of July during the 1980–2023 Period

One of the main factors contributing to the reduction of vegetation cover in the Shirabad neighborhood is widespread and unauthorized construction, coupled with consecutive droughts. Based on the analysis of the Standardized Precipitation Index (SPI), severe droughts occurred in Zahedan during the years 2000, 2020, and 2023, leading to a decline in vegetation cover in the Shirabad area and the degradation of its natural resources. These findings are consistent with those of Negarsh et al. (2019, p. 124), who highlighted the successive droughts in Zahedan and their impact on the region's agriculture and natural resources. In contrast, vegetation cover in the University neighborhood of Zahedan has increased, indicating that unlike Shirabad the green space of the university has been relatively unaffected by the direct impact of drought. This can be attributed to centralized management of the university's green space and the availability of water resources for its maintenance. An analysis of land surface temperature (LST) data in the Shirabad and University neighborhoods shows a notable increase in temperature in recent years. This temperature rise has directly affected the climate resilience of these areas, reducing the capacity of local ecosystems to adapt to environmental changes. A decrease in climate resilience implies a reduction in the regions' ability to cope with environmental challenges such as floods, droughts, and dust storms, which can have serious consequences for the ecosystem and the quality of life of local residents (Sadeghi & Taghvaei, 2024, p. 142).

Neighborhood Vulnerability Ranking Using the TOPSIS Technique

In this study, data related to various vulnerability components were collected and evaluated, and then scored for the University and Shirabad neighborhoods based on the Likert scale. To analyze the level of vulnerability in these areas, four main components were considered. The TOPSIS technique (Technique for Order of Preference by Similarity to Ideal Solution), a widely used multi-criteria decision-making (MCDM) method, was employed to rank the neighborhoods in terms of vulnerability. Since all components in the TOPSIS model must be quantitative, the qualitative data on neighborhood vulnerability were converted into numerical values using the Likert scale, as shown in Table 3. This conversion allowed for accurate and comparable mathematical calculations, thereby enhancing the precision of the final analyses.

Table3. Conversion of Qualitative Components to Quantitative Values

Qualitative Component	Very Low	Low	Medium	High	Very High
Quantitative Equivalent	1	3	5	7	9

(Source: Hosseini et al., 2016, p. 87)

After converting the qualitative data into quantitative values, the initial vulnerability assessment matrix for the two studied neighborhoods was constructed (Table 4). This matrix represents the scores of the main vulnerability components for each neighborhood. The data indicate that the University neighborhood scores higher across all components compared to Shirabad, suggesting that its vulnerability is lower than that of Shirabad.

Table 4. Vulnerability Assessment Matrix for the Studied Neighborhoods

Component	Economic	Social	Environmental	Infrastructure & Institutional
University	7	5	5	5
Shirabad	1	3	1	1

In the next step, the initial data matrix was normalized to enable the calculation of each neighborhood's distance from the positive and negative ideal solutions. The results of this step indicate that the University neighborhood scores significantly higher across all components compared to Shirabad (Table 5).

Table 5. Normalized Vulnerability Assessment Matrix for the Studied Neighborhoods

Component	Economic	Social	Environmental	Infrastructure & Institutional
University	0.98	0.86	0.98	0.98
Shirabad	0.2	0.51	0.2	0.2

In the following stage, the positive and negative ideal solutions were determined for each component (Table 6). Since all components are positive in nature, the highest value in each column was considered the positive ideal solution, while the lowest value was taken as the negative ideal solution. These values served as the basis for calculating the distance of each neighborhood from the ideal condition.

Table 6. Positive and Negative Ideal Solutions

Component	Economic	Social	Environmental	Infrastructure & Institutional
Component Type	Positive	Positive	Positive	Positive
Positive Ideal Solution	0.98	0.86	0.98	0.98
Negative Ideal Solution	0.2	0.51	0.2	0.2

After identifying the ideal solutions, the Euclidean distance of each neighborhood from the positive and negative ideal was calculated, and finally, the relative closeness (C) of each neighborhood to the ideal condition was determined (Table 7). The results indicate that the University neighborhood (C = 1) is the closest to the ideal solution and thus has the lowest vulnerability, while the Shirabad neighborhood (C = 0.01) is the farthest from the ideal indicating higher vulnerability compared to the University area.

Table 7. Distances from Positive and Negative Ideal Solutions and Relative Closeness (C)

Neighborhood	S^+	S^-	C
University	0	1.4	1
Shirabad	1.4	0.01	0.01

By prioritizing the vulnerability components, the University neighborhood ranked first, and Shirabad neighborhood ranked second in terms of alignment with the ideal condition. This study demonstrated that higher resident satisfaction with economic, social, environmental, and infrastructural-institutional components has a direct impact on increasing neighborhood resilience. The results of the TOPSIS technique confirm that the University neighborhood exhibits better social and physical resilience than Shirabad. These findings highlight the infrastructural and social advantages of the University area, likely resulting from greater access to public services, recreational facilities, improved social indicators, and a generally higher quality of life. In contrast, Shirabad suffers from lower resilience due to inadequate infrastructure, economic hardship, and social dissatisfaction. An investigation of the underlying causes of higher vulnerability in Shirabad points to factors such as weak service delivery, informal development, economic constraints, and a lack of effective urban planning all of which contribute to increased vulnerability and reduced resilience. The final analysis emphasizes that attention to economic, social, and infrastructural components plays a key role in enhancing urban resilience. Improving these components not only helps reduce vulnerability but also promotes higher quality of life and sustainable urban development. Indeed, sustainable social development is unattainable without addressing the economic, cultural, value-based, environmental, and technological dimensions. The interactions among social actors, who are the true fabric of urban life, give meaning and depth to sustainable development and enhance the resilience and adaptability of citizens in the face of environmental crises (Nasiri Hendeh Khaleh et al., 2024, p. 164). The findings of this study can serve as a scientific foundation for urban and social planning aimed at reducing neighborhood-level vulnerability.

Discussion and Conclusion

Resilience refers to the ability to adapt to environmental changes and recover after the occurrence of crises. In today's world, where climate change is rapidly impacting communities, the concept of resilience has gained increasing importance. The consequences of these changes such as drought, floods, and rising temperatures have heightened the vulnerability of cities and communities to natural disasters. Additionally, weaknesses in local governance and insufficient preparedness have further complicated crisis management. In many cases, local authorities have failed to implement adequate preventive measures, resulting in substantial human and financial losses. The findings of this study indicate that the University neighborhood, due to its higher vegetation coverage, demonstrates greater resilience to climate change. These results emphasize that green space plays a key role in strengthening urban resilience. Vegetation contributes by absorbing carbon dioxide, producing oxygen, and lowering ambient temperatures, thereby improving air quality and mitigating urban heat island effects. Moreover, vegetation helps retain soil moisture and reduce evaporation, which is critical in mitigating the effects of drought. To enhance Zahedan's resilience to climate change, a comprehensive plan for the development and management of urban green spaces is recommended. Such a plan should include actions such as establishing green belts, expanding parks and public green areas, using drought-resistant plant species, and implementing smart irrigation technologies. Furthermore, citizen participation in the maintenance of green areas and fostering a sense of ownership should be prioritized. Based on the findings of this research and the recognized importance of green space in strengthening resilience, it can be concluded that investing in the development and preservation of urban green spaces is a long-term and profitable investment. This investment not only contributes to improving the quality of life for residents but also strengthens the city's resilience against climate change. In this context, Sadeka et al. (2013, p. 131) highlighted the livelihood vulnerability of communities and proposed diversification as a key strategy for enhancing livelihood resilience. These insights align with the current study, where the differences in resilience between the University and Shirabad neighborhoods suggest that economic and social diversity in the University area may contribute to greater climate adaptability. Similarly, Liebman and Schulte (2015, p. 4) pointed to the role of agricultural diversity in enhancing flexibility in the face of various stresses. In this study, the University neighborhood demonstrated greater flexibility, largely due to its better infrastructure and higher resident awareness of climate-related risks.

References

Adger, W.N, Hughes, T.P, Folke, C., Carpenter, S.R. and Rockström, J. (2005). Social-ecological resilience to coastal disasters. Science, 309(5737), 1036-1039. https://www.science.org/doi/10.1126/science.1112122

Afrakhteh, H., & Hajipour, M. (2024). Food Self-Sufficiency and Water Resources: Returning to Iran's Future Challenge. *Journal of Green Development Management Studies*, 3(2), 43–57. (In Persian). https://doi.org/10.22077/jgdms.2024.3114

Alberti, M. (2005). The effects of urban patterns on ecosystem function. Ecology, 86(8), 1986-1994 . https://doi.org/10.1016/j.landurbplan.2006.08.001

Alijani, B., Mahmoudi, P., & Chougan, A. (2011). Investigating the Trend of Annual and Seasonal Rainfall Changes in Iran Using Non-Parametric Methods. *Climate Research Studies*, 3(9), 23–42. (In Persian). https://www.sid.ir/paper/401943/fa

Chen, X, Wang, H, Lyu, W. (2022). The Mann-Kendall-Sneyers test to identify the change points of COVID-19 time series in the United States. BMC Medical Research Methodology, 22(1), 233-247. https://doi.org/10.1186/s12874-022-01714-6

Eskandari Sani, M., Alizadeh, M., & Rezaei Nasab, A. (2023). Investigating the Social Effects of Urban Green Space Development in Quchan. *Journal of Green Development Management Studies*, 2(2), 88–102. (In Persian). https://doi.org/10.22077/jgmd.2023.6669.1039

Ferrini, F, Fini, A, Mori, J, & Gori, A. (2020). Role of Vegetation as a Mitigating Factor in the Urban Context. Sustainability, 12(10), 4247. 1-22. https://doi.org/10.3390/su12104247

Gadedjisso-Tossou, A, et al. (2021). Rainfall and temperature trend analysis by Mann–Kendall test and significance for rainfed cereal yields in northern Togo. Climate, 9(3), 1-21. https://doi.org/10.3390/sci3010017

Gherri, B. (2023). The Role of Urban Vegetation in Counteracting Overheating in Different Urban Textures. Land, 12(12), 1-15. https://doi.org/10.3390/land12122100

Golestani, Z., Mohammadi, H., Borna, R., & Asadian, F. (2022). Analysis of the Relationship Between Land Surface Temperature and Vegetation Cover in the Formation of Urban Heat Islands and Its Hazards (Case Study: Isfahan Metropolis). *Environmental Hazards Management*, 9(4), 341–354. (In Persian). https://doi.org/10.22059/jhsci.2023.349481.749

Gonzalo R. Arce. (2004). Nonlinear Signal Processing: A Statistical Approach, John Wiley & Sons, First published. 1 -459.https://doi.org/ doi:10.1002/0471691852

Guttman, N. B. (1999). Accepting the standardized precipitation index: A calculation algorithm. Journal of the American Water Resources Association, 35(2), 311-322. https://doi.org/10.1111/j.1752-1688.1999.tb03592.x

Hao, F, Zhang, X, Ouyang, W, Skidmore, A. K, Toxopeus, A. G. (2012). Vegetation NDVI Linked to Temperature in the Upper Catchments of Yellow River. Environmental Modeling & Assessment, 17, 389-398 . https://doi.org/10.1007/s10666-011-9297-8

Helsel, D.R, Hirsch, R.M, Ryberg, K.R., Archfield, S.A, and Gilroy, E.J, 2020, Statistical methods in water resources: U.S. Geological Survey Techniques and Methods, book 4, chap. A3, 458. https://doi.org/10.3133/tm4a3.

Hesari, P. (2023). Assessing the Adequacy of Green Space Allocation in the Detailed and Executive Plan of District 22, Tehran. *Green Development Management Studies*, 2(2), 67–87. (In Persian). https://doi.org/10.22077/jgdms.2024.7078.1051

Hosseini Chamani, F., Farkhiyan Firoozi, A., & Amerikhah, H. (2019). Transfer Function for Estimating Soil Moisture Using Vegetation Indices, Soil Surface Temperature, and the Normalized Moisture Index. *Journal of Soil and Water Conservation Research*, 26(4), 239–254. (In Persian). https://doi.org/10.22069/jwsc.2019.15306.3053

Hosseini, S., Oladi, J., & Amirnejad, H. (2015). Prioritizing Ecological, Economic, and Social Indicators of National Parks Using Multi-Criteria Decision-Making Techniques (Entropy, SAW, and TOPSIS). *Journal of Wood and Forest Science and Technology Research*, 22(4), 1–28. (In Persian). https://jwfst.gau.ac.ir/article_2821.html

Khosravi Yeganeh, S., Karampour, M., & Nasiri, B. (2024). Assessing the Impact of Drought on Vegetation Cover in Iran Using Satellite Imagery and Meteorological Data. *Iranian Journal of Remote Sensing and GIS*, 16(1), 81–102. (In Persian). https://doi.org/10.48308/gisj.2023.103394

Landry, S. M, & Chakraborty, J. (2009). Street Trees and Equity: Evaluating the Spatial Distribution of an Urban Amenity. Environment and Planning A, 41(11), 2651-2670. https://doi.org/10.1068/a41236

Liebman, M, & Schulte, L. A. (2015). Enhancing agroecosystem performance and resilience through increased diversification of landscapes and cropping systems. Elementa: Science of the Anthropocene, 3(1), 1-7.https://doi.org/10.12952/journal.elementa.000041

Makari, M., & Abbasnia, M. (2020). Analysis of Maximum Temperature Trends Using Mann-Kendall and Spearman Tests in Various Regions of Iran. *Nivar*, 44(108–109), 33–47. (In Persian).https://doi.org/10.30467/nivar.2020.211885.1143

Malekan, A., Dadvar Khani, F., & Darban Astaneh, A. (2020). Drought Management in Rural Areas with Emphasis on Resilience Approach (Case Study: Kermanshah's Kangavar County). *Human Geography Research*, 2(53), 717–732. (In Persian). https://doi.org/10.22059/jhgr.2021.310008.1008169

Manouchehri, E., Mohammadpour, S., Hataminejad, H., & Hesam, M. (2011). Evaluation and Recommendation of Criteria and Standards for Urban Green Space Development Planning. *Geographical Research*, 102, 25–50. (In Persian). https://journals.ui.ac.ir/article_17900.html

McKee, T. B, Doesken, N. J, & Kleist, J. (1993). The relationship of drought frequency and duration to time scales. Proceedings of the 8th Conference on Applied Climatology, 17(22), 179-183.http://clima1.cptec.inpe.br/~rclima1/pdf/paper_spi.pdf

McKee, T. B, Doesken, N. J, & Kleist, J. (1995). Drought monitoring with multiple time scales. 9, 233–236. https://ci.nii.ac.jp/naid/10028178079/

McPhearson T, Karki M, Herzog C, et al. Urban Ecosystems and Biodiversity. In: Rosenzweig C, Solecki WD, Romero-Lankao P, Mehrotra S, Dhakal S, Ali Ibrahim S, eds. Climate Change and Cities: Second Assessment Report of the Urban Climate Change Research Network. Cambridge University Press; 2018:257-318. https://doi.org/10.1017/9781316563878.015

Mileti, D. S. (1999). Disasters by design: A reassessment of natural hazards in the United States. Washington, DC: Joseph Henry Press), 1-371. https://doi.org/10.17226/5782

Najafi, Z., Darvish Safat, A. A., Fatehi, P., & Atarod, P. (2020). Analyzing the Dynamics of Vegetation Cover Using Landsat Satellite Images in the Tehran Metropolis. *Iranian Journal of Forest*, 12(2), 257–270. (In Persian). https://www.ijf-isaforestry.ir/article_114056.html

Nasiri Hendehkhaleh, E., Esmaeili, F., Alizadeh Zonouz, M., & Rajabi Kalvani, A. H. (2024). The Role of Physical-Environmental Components in Social Sustainability in Ban Borz Neighborhood of Ilam City. *Green Development Management Studies*, 3(1), 161–176. (In Persian). https://doi.org/10.22077/jgdms.2024.7302.1080

Negarish, H., Khosravi, M., Shah Hosseini, M., & Mahmoudi, P. (2010). A Study of Short-Term Droughts in Zahedan County. *Geography and Development*, 8(18), 109–134. (In Persian). https://doi.org/10.22111/gdij.2010.1123

Norouzi, A. (2019). Assessing the Resilience of Rural Settlements Against Environmental Hazards (Case Study: Boldaji District). *Physical Spatial Planning*, 4(3), 73–88. (In Persian). https://doi.org/10.30473/psp.2019.6390

Nowak, U, & Crane, D. E. (2002). The urban forest effects: A guide to urban forestry research. USDA Forest Service, General Technical Report, 714-720. https://research.fs.usda.gov/treesearch/18420

Parry, M, Arnell, N, Berry, P, Dodman, D, Fankhauser, S, Hope, C, Kovats, S, Nicholls, R, Satterthwaite, D, Tiffin, R, & Wheeler, T. (2009). Assessing the Costs of Adaptation to Climate Change: A Review of the UNFCCC and Other Recent Estimates. London: International Institute for Environment and Development (IIED) and Grantham Institute for Climate Change, 1-117. https://doi.org/10.1080/00139150903337423

Poudineh, M.R., Heidarinia, M., Mousavi, S.R., & Doosti Moghaddam, H. (2020). Monitoring Drought Indices in Zahedan City Across Different Time Periods. *Physical Geography*, No. 37, 133–143. (In Persian). https://journals.iau.ir/article_676562.html

Sadeghi, H., & Taghvaei, M. (2024). Analysis of Environmental Data in the Establishment and Sustainable Development of Rural Settlements in Isfahan County Using Geographic Information Systems (GIS). *Journal of Green Development Management Studies*, 3(1), 135–160. (In Persian). https://doi.org/10.22077/jgdms.2024.7215.1074

Sadeka, S, Karim, R, Rahman, M. M, & Islam, M. R. (2013). Livelihood vulnerability due to disaster: Strategies for building disaster resilient livelihood. Retrieved from , 127-133. https://www.researchgate.net/publication/259922125

Sarani, M., & Hashemi, Z. (2023). Investigating the Relationship Between Hydrological Drought and Vegetation Cover Using Landsat Imagery in the Eastern Part of the Sistan Region. *Natural Environmental Hazards*, 38, 75–96. (In Persian). https://doi.org/10.22111/jneh.2023.44340.1938

Shahabfar, A, & Eitzinger, J. (2013). Spatio-Temporal Analysis of Droughts in Semi-Arid Regions by Using Meteorological Drought Indices. Atmosphere, 4(2), 94-112. https://doi.org/10.3390/atmos4020094

Sullivan, C. & Meigh, J. (2005). Targeting attention on local vulnerabilities using an integrated index approach: the example of the climate vulnerability index. Water Science and Technology, 51 (5), 69-78. https://doi.org/10.2166/wst.2005.0111

Yadegari Far, F., Poudineh, M. R., & Esmaeil Nejad, M. (2023). Assessment of the Resilience of Zahedan County Against Water Crisis and Drought. *Applied Researches in Geographical Sciences*, 23(68), 345–364. (In Persian). http://jgs.khu.ac.ir/article-1-3573-fa.html

Zhang, D, Yao, M, Chen, Y, & Liu, Y. (2025). The Role of Urban Vegetation in Mitigating Fire Risk Under Climate Change: A Review. Sustainability, 17(6), 2680. 1-25. https://doi.org/10.3390/su17062680